NUMERICAL SIMULATION OF SALINITY DISTRIBUTIONS IN THE YATSUSHIRO SEA BY POM COMBINED WITH WATERSHED MODEL FOR B-CLASS RIVER BASIN

Sha Lou[1], Akihide Tada[2], Akira Tai[3], Shinichiro Yano[4], Seiji Suzuki[5] and Shuguang Liu[6]

[1]Dept. of System Science, Graduate School of Science and Technology, Nagasaki University, lousha19@gmail.com
[2]Division of System Science, Graduate School of Engineering, Nagasaki University, atada@nagasaki-u.ac.jp
[3]Institute for Advanced Study, Kyushu University, tai@civil.kyushu-u.ac.jp
[4]Dept. of Urban and Environmental Engineering, Faculty of Engineering, Kyushu University, yano@civil.kyushu-u.ac.jp
[5]Division of System Science, Graduate School of Engineering, Nagasaki University, ssuzuki@nagasaki-u.ac.jp
[6]Dept. of Hydraulic Engineering, Tongji University, liusgliu@tongji.edu.cn

Minamata Bay, located in the southeast coastal areas of the Yatsushiro Sea, was heavily polluted due to the discharge of organic mercury compound from a chemical factory since 1932. Some research has demonstrated that correlations between seawater characteristics and methyl-mercury concentration are observed. Based on the analysis of low-salinity water masses in the Yatsushiro Sea, this paper deals with salinity field in the Yatsushiro Sea under the effect of freshwater from rivers by Princeton Ocean Model (POM) combined with watershed model. Firstly POM is established covering both the Yatsushiro Sea and the Ariaka Sea. Salinity fields in six cases are calculated under freshwater inflow from a A-Class river: the Kuma River. Then a watershed model is applied in basin of a B-Class river: the Komenotsu River for Case5 and Case6. Rainfall data and physical characteristics of catchment are utilized to estimate river's discharge by Kinematic Wave Method (KWM). Through the computation, it's indicated that simulated salinities in surface layer exhibit the same trends as the measured ones at most cases. The deviations in Case1-Case4 are less than 20% at most areas, but the deviations become obviously higher in Case5 and Case6 when the measured salinities are lower than 5 and the highest deviations always occur in surface layer. Adding the Komenotsu River's discharges into POM, salinities at two stations (St.25 and St.26) in Case5 and one station (St.26) in Case6 have decreased owing to the rainfall and closer location to the river mouth.

Key Words **:** *the Yatsushiro Sea, salinity filed, freshwater inflow, POM, kinematic wave method*

1. INTRODUCTION

Minamata Bay, located in the southeast coastal areas of the Yatsushiro Sea, was heavily polluted due to the discharge of organic mercury compound from a chemical factory since 1932. Besides control of the pollution, many observation measures have also been implemented (Kumagai et al., 1978; Tomiyasu et al., 2000; Tomiyasu et al., 2008). Although at present further research still needs conducting to comprehensively understand the dynamic behavior of mercury in Minamata Bay, some research has demonstrated that correlations between seawater characteristics and methyl-mercury concentration are observed (Matsuyama et al., 2011). However, salinity is always studied for red tide or algae bloom in the Yatsushiro Sea (Iunoe et al., 2007; Tomoyuki et al., 2009; Murata et al., 2009), only a few research in respect of flow pattern and runoff have been done.

In 2011, low-salinity water masses are analyzed in the Yatsushiro Sea based on six years' measured data between 1979 and 1998 (Tai et al., 2011). Salinities in the Yatsushiro Sea were measured at 20 stations (**Fig.1**) and in six vertical layers: L-S0, L-S05, L-S10, L-S20, L-S30, L-SB (water surface;

5m, 10m, 20m and 30m below water surface; bottom). On this condition, this paper deals with salinity field in the Yatsushiro Sea under the effect of fresh water from rivers by numerical simulation.

2. NUMERICAL SIMULATION BY POM

Many numerical models have been used to simulate salinity field in the ocean (Vinayachandran et al., 2009; Kitazawa et al., 2011; Iakovlev, 2012). In this paper, Princeton Ocean Model (POM), developed in Princeton University (Mellor, 2004), is applied to reproduce the salinity filed in the Yatsushiro Sea. It has been widely utilized in the world (Roed et al., 2007, Aschariyaphotha et al., 2008). The basic equations are shown in Eq. (1)~(4).

$$\frac{\partial DU}{\partial x}+\frac{\partial DV}{\partial y}+\frac{\partial \omega}{\partial \sigma}+\frac{\partial \eta}{\partial t}=0 \tag{1}$$

$$\frac{\partial DU}{\partial t}+\frac{\partial DU^2}{\partial x}+\frac{\partial DUV}{\partial y}+\frac{\partial U\omega}{\partial \sigma}-fVD+gD\frac{\partial \eta}{\partial x} +\frac{gD^2}{\rho_0}\int_\sigma^0[\frac{\partial \rho'}{\partial x}-\frac{\sigma'}{D}\frac{\partial D}{\partial x}\frac{\partial \rho'}{\partial \sigma'}]d\sigma'=\frac{\partial}{\partial \sigma}[\frac{K_M}{D}\frac{\partial U}{\partial \sigma}]+F_x \tag{2}$$

$$\frac{\partial DV}{\partial t}+\frac{\partial DUV}{\partial x}+\frac{\partial DV^2}{\partial y}+\frac{\partial V\omega}{\partial \sigma}+fUD+gD\frac{\partial \eta}{\partial y} +\frac{gD^2}{\rho_0}\int_\sigma^0[\frac{\partial \rho'}{\partial y}-\frac{\sigma'}{D}\frac{\partial D}{\partial y}\frac{\partial \rho'}{\partial \sigma'}]d\sigma'=\frac{\partial}{\partial \sigma}[\frac{K_M}{D}\frac{\partial V}{\partial \sigma}]+F_y \tag{3}$$

$$\frac{\partial DS}{\partial t}+\frac{\partial DUS}{\partial x}+\frac{\partial DVS}{\partial y}+\frac{\partial \omega S}{\partial \sigma}=\frac{\partial}{\partial \sigma}[\frac{K_H}{D}\frac{\partial S}{\partial \sigma}]+F_S \tag{4}$$

where U, V are the horizontal velocities, ω is sigma coordinate vertical velocity, S is salinity, η is the surface elevation, H is bottom topography and $D=H+\eta$.

The model is established covering all the Yatsushiro Sea and the Ariake Sea (**Fig.1**). Number of horizontal grids is 438 × 468 with 10' interval in both longitude and latitude, and there are ten layers in vertical direction. Open boundary is given at the southern end of the simulation area using lunar semi-diurnal tide constituent of tidal motion (M_2 with amplitude of 1.0m). Time interval of external mode is 1s and that of internal mode is 5s. Ten layers in the model are divided into three parts roughly: surface-water, middle-water and bottom-water for setting the vertical initial conditions of salinity and temperature. Initial conditions of surface-water and bottom-water are interpolated directly from measured data at layers: L-S0 and L-SB, respectively, while for middle-water it is interpolated from averaged measured data of Layer S05, S10, S20, S30. Horizontal initial conditions of three parts are interpolated from measured salinity at 20 stations as shown in eq.(5). Real-time discharge of the Kuma River (A-Class) is specified as the freshwater inflow. Other calculation conditions are shown in **Table 1**.

$$S_{i,j}=\sum_{n=1}^{n_{max}}(S_n/L_n^{i,j})/\sum_{n=1}^{n_{max}}(1/L_n^{i,j}) \tag{5}$$

where n_{max} is the total number of measured stations, S_n stands for measured salinity or temperature at Station n, $L_n^{i,j}$ means distance between Station n and grid *(i,j)* in numerical model, $S_{i,j}$ is the salinity or temperature at grid *(i,j)* in numerical model.

Verification of the flow field by POM has been carried out at three stations in the Ariake Sea and two stations in the Yatsushiro Sea including one station at Minamata Bay as mentioned in (LOU et al., 2011).

Fig.2 is the comparisons of measured and simulated surface layer's salinity at 20 stations in Case1-Case6. The simulated salinity is the averaged data at the last day of the calculation. The figure shows simulated salinities in surface layer exhibit the same trends as the measured ones at most cases and the magnitudes have slight difference except that at St.26 in Case2. The extreme low measured salinity at St.26 must be caused by measurement error. In Case3 and Case4, simulated salinities at St.40 are much higher than the measured data. St.40 is located around the mouth of the Kuma River. The influence of freshwater might be more significant than the calculation. Severe deviations appear in the northern part of Case5 and in the south-central part of Case6. And most of these stations (St.23, 24, 25, 26, 28) are just directed toward mouth of the Komenotsu River.

Fig.3 shows the depth profiles of measured salinity, simulated salinity and the deviation. It's

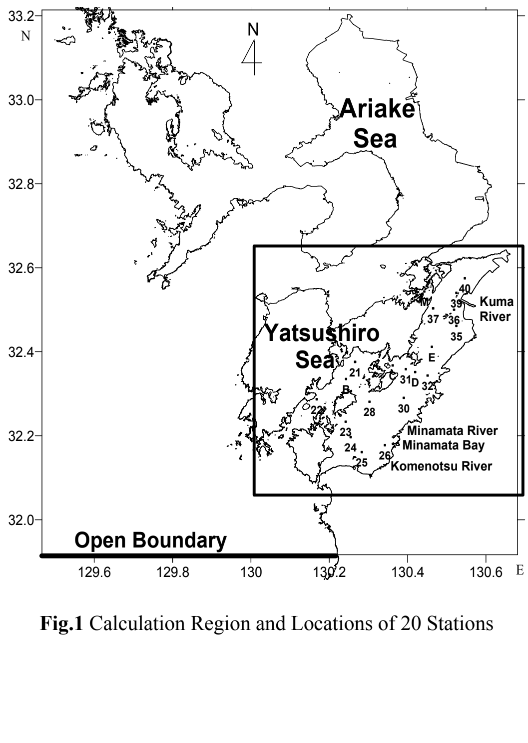

Fig.1 Calculation Region and Locations of 20 Stations

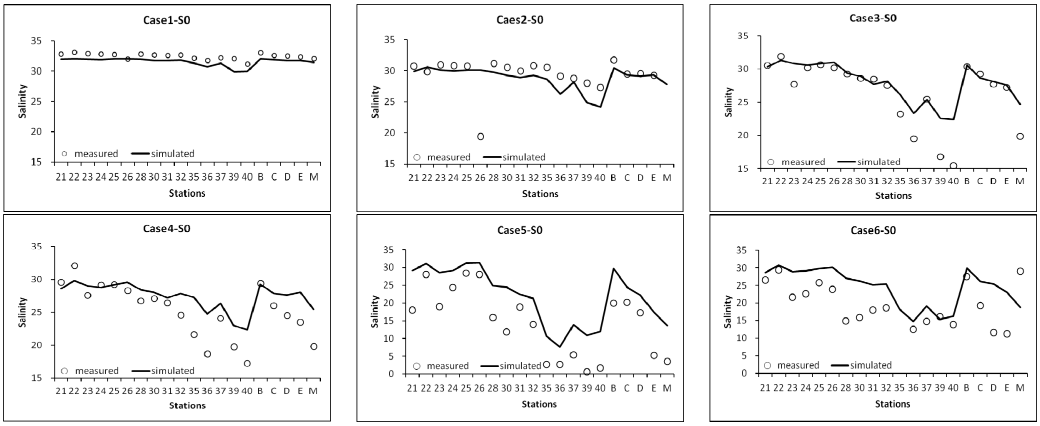

Fig.2 Comparisons of Measured and Simulated Salinity at 20 stations in Six Cases

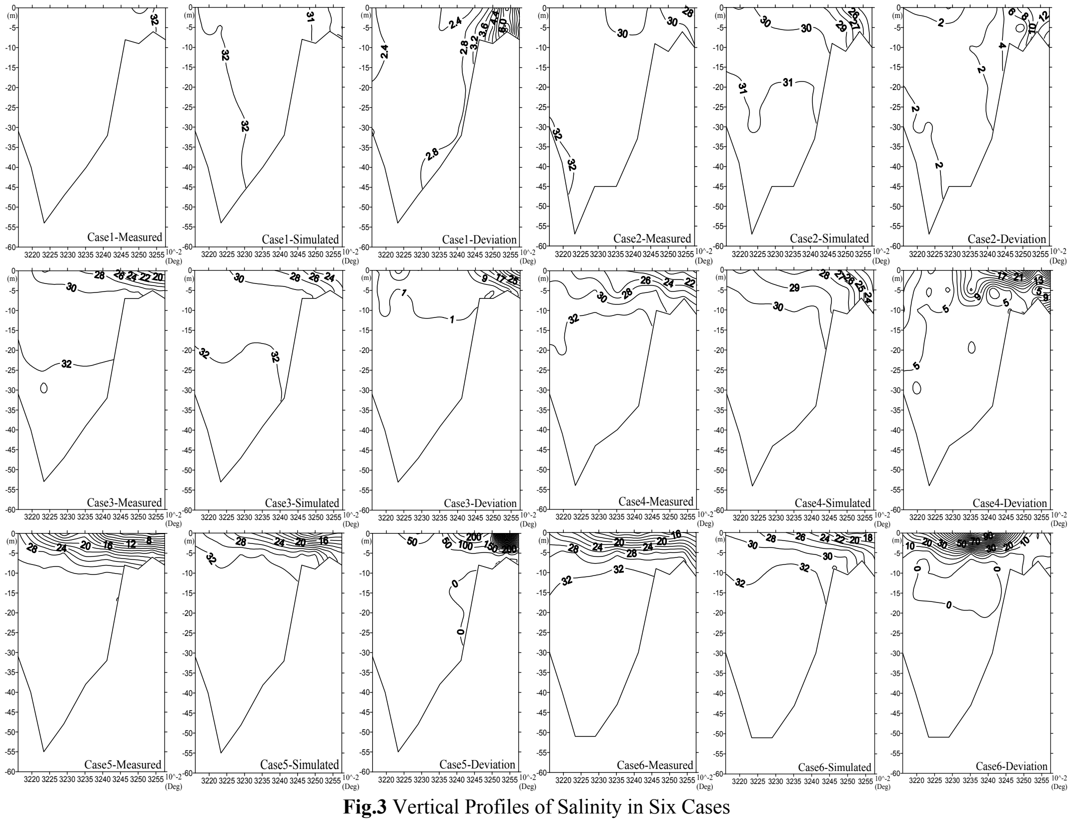

Fig.3 Vertical Profiles of Salinity in Six Cases

(X-Axis: latitude; Y-Axis: water depth; Deviation =100*|Simulated - Measured |/ Measured)

realized that the tendency of simulated salinities are in accord with the measured data in not only the horizontal but also the vertical distribution, and the deviations in Case1-Case4 are less than 20% at most areas (except 40% in northern part in Case3). But the highest deviations reach up to 1600% and 100% in Case5 and Case6 respectively when the measured salinities are no greater than 12. In addition, the deviations are always higher on the surface layer.

Table1 Calculation Conditions for Salinity Fields in Six Cases

No.	Initial Time	End Time	Calculation Time
Case1	25th Aug.	24th Sep.	31 Days in 1998
Case2	14th Aug.	10th Sep.	28 Days in 1980
Case3	18th Jun.	23rd Jul.	36 Days in 1996
Case4	28th Jun.	25th Jul.	28 Days in 1979
Case5	13rd Jun.	6th Jul.	24 Days in 1995
Case6	24th Jun.	22nd Jul.	29 Days in 1982

3. WATERSHED MODEL

Based on the results of POM, it's indicated that improvement is necessary for Case5 and Case6. Although there is lack of discharge data of B-Class river, the Komenotsu River which pours into the sea at the southern areas should be considered to consistent with practical situation. Therefore, a watershed model using Kinematic Wave Method (Wooding, 1965; Wong et al., 1989; Suzuki et al., 2011) is adopted in basin of the Komenotsu River whose mouth is located in Izumi, Kagoshima Prefecture. The river's discharge is related to rainfall and physical characteristics of catchment such as areas, slope and surface roughness. The whole basin would be ideally divided into several elements composed of a river channel and two catchments in KWM. Basic equations are as following.

For the catchment:

$$\frac{\partial h}{\partial t}+\frac{\partial q}{\partial x}=r_e \tag{6}$$

$$h=Kq^P \tag{7}$$

$$P=\frac{3}{5} \tag{8}$$

$$K=\left(\frac{n}{\sqrt{i}}\right)^P \tag{9}$$

For the river channel:

$$\frac{\partial A}{\partial t}+\frac{\partial Q}{\partial x}=2q \tag{10}$$

$$A=KQ^P \tag{11}$$

$$P=\frac{3}{2Z+3} \tag{12}$$

$$K=\left(\frac{n}{k_1^{2/3}\sqrt{i}}\right)^P \tag{13}$$

in which A is the channel flow area, Q is the channel discharge, h is the depth of flow, q is the discharge per unit width, t is the time, x is the distance along the catchment or channel in the direction of flow, r_e is the rainfall excess, n is the roughness of underlying surface, i is slop, and k_1 and Z are the parameters relating to the flow area and flow depth.

Fig.4 is about 73 river channels with 146 catchments under different land-use in the Komenotsu Basin. In every segment, the length interval is 10m and the time step is one hour. **Fig.5** shows the rainfall data and discharge results of the Komenotsu River in Case5 and Case6. The rainfall data is averaged from data at three meteorological stations in Kagoshima Prefecture: Izumi, Ookuchi and Shibisan. The maximum instantaneous rainfall is around 31mm/h in both Case5 and Case6, but the accumulated rainfall is 767mm in Case5 and 536mm in Case6. Through the utilization of watershed model for the Komenotsu River, a discharge of approximately 700 m^3/s is caused by large amount of rainfall in Case5, while in Case6 the maximum discharge is only 300 m^3/s.

Adding the discharges of the Komenotsu River into POM as a boundary condition, improved results of the salinity distribution for Case5 and Case6 are illustrated in **Fig.6**. Obvious decreases of salinity at St.25 and St.26 occur in Case5. From the locations of 20 stations in **Fig.1**, it's found out St.25 and St.26 are much closer to the Komenotsu River's mouth than other stations. Even with the abundant precipitation as in Case5, freshwater from the Komenotsu River only has some influence in certain areas around river mouth. And in Case6 under the relatively lower rainfall, only salinity at St.26 has been slightly impacted by the Komenotsu River.

4. CONCLUSIONS

Through the analysis of measured and simulated salinity fields in the Yatsushiro Sea, several conclusions have been summarized as following:

(1) In six cases which are all in summer season, salinity stratification is observed in evidence and the measured salinities are lower in the surface layer. But at some stations, the measured surface layer's salinities are relatively low like 19.4 at St.26 in Case2, 11.63 at St.D and 11.16 at St.E in Case6, moreover, salinities at some stations in Case5 are lower than 5 which cause 1600% deviation in **Fig.3**. Reliability of measured data should be confirmed.

(2) POM could describe salinity field in the Yatsushiro Sea with a certain accuracy. Mostly, simulated salinities agree with the measured data quite well. But around the Kuma River's mouth and in the southern part, the simulated salinities are higher than the measured ones. Deviations reduce with the increasing of water depth.

(3) KWM is a valid method for the watershed model to estimate river's discharge. Considering the

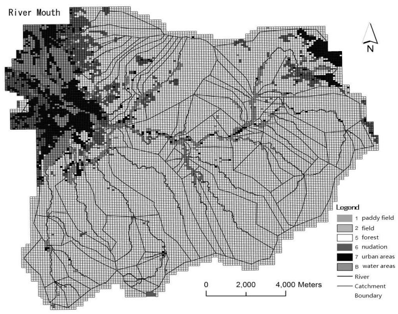

Fig.4 Land-use in the Komenotsu Basin

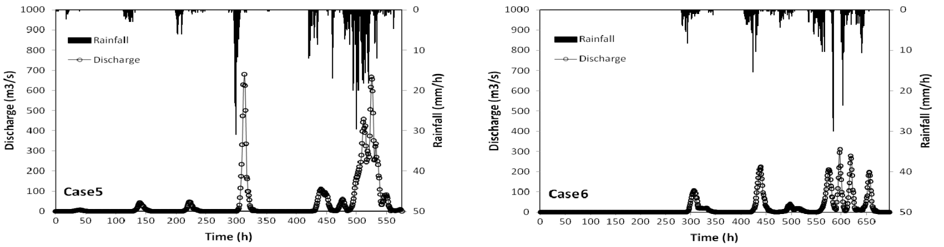

Fig.5 Rainfall Data and Discharge of the Komenotsu River in Case5 and Case6

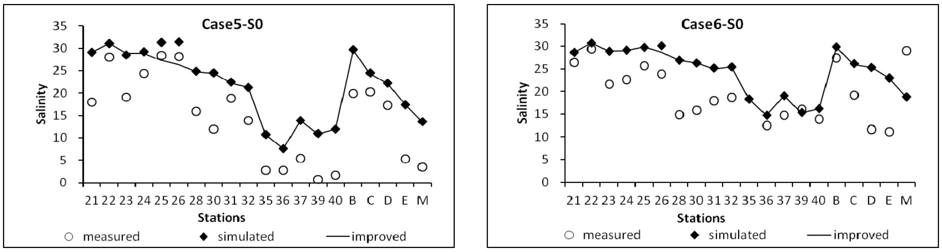

Fig.6 Improved Results of Salinity Distribution by Watershed Model using KWM in Case5 and Case6

freshwater from the Komenotsu River, little impact has appeared around river mouth areas in Case5 and Case6 under the precipitation.

Therefore, to heighten the accuracy, more researches still need to be done, such as considering other B-Class rivers or scaling down the model.

REFERENCES

Aschariyaphotha, N., Wongwises, P., Wongwises, S., Humphries, U. W., and You, X. B. (2008): *Simulation of Seasonal Circulations and Thermohaline Variabilities in the Gulf of Thailand*, Advances in Atmospheric Sciences, Vol. 25, No. 3, pp. 489-506.

Iakovlev, N. G. (2012): *On the Simulation of Temperature and Salinity Fields in the Arctic Ocean*, Atmospheric and Oceanic Physics, Vol. 48, No. 1, pp. 86-101.

Inoue, Y., Miyasaka, J., Ono, T., and Ihn, H. (2007): *The growth of Vibrio vulnificus and the habitat of infected patients in Kumamoto*, Bioscience trends, Vol. 1, No. 3, pp. 134-139.

Kitazawa, D., and Yang, J. (2012): *Numerical analysis of water circulation and thermohaline structures in the Caspian Sea*, Journal of Marine Science and Technology, No. 1, pp. 1-13.

Kumagai, M., and Nishimura, H. (1978): *Mercury distribution in seawater in Minamata Bay and the origin of particulate mercury*, Journal of the Oceanographical Society of Japan, Vol. 34, pp. 50-56.

Lou, S., Tada, A., Ishihara, T., Tai, A., and Yano, S. (2011): *Numerical analysis on characteristics of flow current in Yatsushiro Sea and Ariake Sea*, Proceedings of the Thirteenth International Summer Symposium, JSCE, pp. 139-142.

Matsuyama, A., Eguchi, T., Sonoda, I., Tada, A., Yano, S., Tai, A, Marumoto, K., Tomiyasu, T., and Akagi, H. (2011): *Mercury speciation in the water of Minamata Bay, Japan*, Water Air Soil Pollution, No. 218, pp. 399-412.

Mellor, G. L. (2004): *Users guide for a three-dimensional primitive equation numerical ocean model*, Manual of Princeton Ocean Model.

Murata, K., and Sakurada, K. (2009): *The growth environment and reaction to Cochlodinium polykrikoides red tides in the Yatsushiro Sea*, Bulletin of the Plankton Society of Japan, Vol. 56, No. 1, pp. 52-55 (in Japanese).

Roed, L. P., and Albretsen J. (2007): *The impact of freshwater discharges on the ocean circulation in the Skagerrak/ northern North Sea area Part I: model validation*, Ocean Dynamics, No. 57, pp. 269-285.

Suzuki, S., Tada, A., Nishida, W., and Sakaguchi, M. (2011): *Study on the Characteristics of Flow Structure and Water Quality in the Imari Bay by means of Numerical Model taking account of River Loads*, Journal of Japan Society of Civil Engineers, Ser. B2 (Coastal Engineering). Vol. 67, No. 2, pp. I_831-I_835 (in Japanese).

Tai, A., Yano, S., Tada, A., Kamikubo, Y., Yano, K., Saita, T., Hashimoto, A., and Ishihara T. (2011): *Low-Salinity Water Masses in Summer and the Change of Tidal Current by Past Coastline Transition in the Yatsushiro Sea*, Journal of Japan Society of Civil Engineers, Ser. B2 (Coastal Engineering), Vol. 67, No. 2, pp. I_341-I_345 (in Japanese).

Tomiyasu, T., Matsuyama, A., Eguchi, T., Marumoto, K., Oki, K., and Akagi, H. (2008): *Speciation of mercury in water at the bottom of Minamata Bay, Japan*, Marine Chemistry, No. 112, pp. 102-106.

Tomiyasu, T., Nagono, A., Yonehara, N., Sakamoto, H., Rifardi, Oki, K., and Akagi,H. (2000): *Mercury contamination in the Yatsushiro Sea, south-western Japan: spatial variations of mercury in sediment*, The Science of the Total Environment, No.257, pp. 121-132.

Tomoyuki, S., Kiyonari, S., Yusuke, J., Masashi, O., et al. (2010): *Effects of temperature, salinity and light irradiance on phytoplankton growth in the Yatsushiro Sea*, Nippon Suisan Gakkaishi, Vol. 76, No. 1, pp. 34-45 (in Japanese).

Vinayachandran, P. N., and Nanjundiah, R. S. (2009): *Indian Ocean sea surface salinity variations in a coupled model*, Climate Dynamics, No.33, pp. 245-263.

Wong T. S. W., and Chen C.N. (1989): *Use of kinematic wave method to assess effects of urban development on flood peak changes*, Proceedings of the Baltimore Symposium, pp.93-101.

Wooding R. A. (1965): *A hydraulic model for the catchment-stream problem: I. Kinematic-wave theory*, Journal of Hydrology, No.3, pp. 254-267.

(Received June 15, 2012)